Optical Spectroscopy of Single Crystal [Re(bpy)(CO)$_4$](PF$_6$): Mixing between Charge Transfer and Ligand Centered Excited States

Geoffrey F. Strouse* and Hans U. Güdel*

Institut für anorganische Chemie, Universiät Bern, Freiestrasse 3, 3000 Bern 9, Switzerland

Valerio Bertolasi and Valeria Ferretti

Dipartimento di Chimica, Universita di Ferrara, Via L. Borsari, 46, 44100 Ferrara, Italy

Received May 19, 1995[⊗]

The photochemical, photocatalytic, and luminescent properties of d^6 transition metal complexes are dictated by the character of the lowest electronic transition. Observation of the lowest excited electronic state in single crystal [Re(bpy)(CO)$_4$](PF$_6$) by high resolution absorption spectroscopy at cryogenic temperatures allows assignment as a nominally ^{3}LC transition with its electronic origin centered at 22 510 cm^{-1}. Mixing between the ligand centered and charge transfer excitations in transition metal complexes can significantly effect the optical spectroscopy and decay processes of the complex. The ^{3}LC state is weakly mixed (3%) with the lowest lying ^{1}CT state (31 570 cm^{-1}), resulting in the observation of metal−ligand vibrational side bands, a shortened luminescence decay (τ = 33.0 μs), and a large zero-field splitting (ZFS) of the electronic origin (ZFS = 7.2 cm^{-1}). These observations are interpreted using a mechanism in which the coupling arises from a large spin−orbit coupling matrix element ($\langle|H_{so}|\rangle$ = 261 cm^{-1}). The presence of a low lying ligand field state can be definitely ruled out from the observed absorption and luminescence behavior. The observed photochemical properties are likely due to the charge transfer character of the first excited state.

1. Introduction

Interest in d^6 transition metal coordination complexes has increased phenomenally in the past decade due to their ability to act as photosensitizers in photoinduced electron transfer or photocatalytic processes.[1−4] The photoredox properties of these materials can be strongly influenced by the nature of the lowest excited state, which may be tuned by the appropriate selection of the chelating ligands.[1] In d^6 transition metal complexes of the type [M(bpy)(CO)$_4$] (M = Cr^0, Mo^0, W^0, Mn^I, Re^I; bpy = 2,2′-bipyridine) few complexes have been found to emit light at room temperature.[5−8] The lowest electronic transition is quite often assigned to metal-to-ligand charge transfer (CT) dπ_M → π^*_L, ligand centered (LC) π → π^*, or ligand field excitations (LF) dπ_M → dσ^*_M, based upon either the dipole strength of the transitions or a luminescence band shape analysis of solutions or solution glasses resulting in a qualitatative rather than quantitative description of the lowest excited state. Band shape analysis of solutions at room temperature or glasses at cryogenic temperatures can be strongly influenced by inhomogeneous broadening in the vibrational progressions of the transitions, therefore limiting the available information content for the electronic transitions. In the [M(bpy)(CO)$_4$] complexes (where M = Cr^0, Mo^0, W^0, Mn^I), which have C_{2v} symmetry, the metal-to-ligand charge transfer state is normally the lowest excited electronic state with a close-lying ligand field state at higher energy.[5] Much attention has been focused on understanding the photophysical properties resulting from the interplay of the two electronic transitions. Assignment of the lowest electronic level can be difficult, and arbitrarily assigned states are misleading for the development of photoinitiated catalysts and interpreting the excited state properties. High resolution crystal spectroscopy at cryogenic temperatures using polarized light allows more detailed characterization of the lowest excited state through the interpretation of intensity and vibrational progressions which are obscured by inhomogeneous broadening in noncrystalline samples.

Electronic origins and vibrational progressions of the lowest electronic transition in Ir^{III}, Rh^{III}, Ru^{II}, and Os^{II} bipyridyl complexes in the solid state have been determined by high

[⊗] Abstract published in *Advance ACS Abstracts*, September 1, 1995.

(1) (a) Juris, A.; Balzani, V.; Barigelletti, F.; Campagna, S.; Belser, P.; Von Zelwesky, A. *Coord. Chem. Rev.* **1988**, *84*, 85. (b) Krause, R. A. *Struct. Bonding (Berlin)* **1987**, *67*, 1. (c) Meyer, T. J. *Pure Appl. Chem.* **1986**, *58*, 1576. (d) Sutin, N.; Creutz, C. *Pure Appl. Chem.* **1980**, *52*, 2717. (e) Meyer, T. J. *Acc. Chem. Res.* **1989**, *22*, 163.

(2) (a) Leasure, R. M.; Sacksteader, L. A.; Nesselrodt, D.; Reitz, G. A.; Demas, J. N.; Degfraff, B. A. *Inorg. Chem.* **1991**, *30*, 3722. (b) Chen, P. Y.; Duesing, R. D.; Graff, D.; Meyer, T. J. *J. Phys. Chem.* **1991**, *95*, 5850 (c) Creutz, C.; Chou, M.; Netzel, L.; Okumura, M.; Sutin, N. S. *J. Am. Chem. Soc.* **1980**, *102*, 1309. (d) Lee, E. J.; Wrighton, M. S. *J. Am. Chem. Soc.* **1991**, *113*, 8562 (e) Cooley, L. F.; Larson, S. C.; Elliott. C. M.; Kelly, D. F. *J. Phys. Chem.* **1991**, *95*, 10694.

(3) (a) Ohno, T.; Yoshimura, A.; Prasad, D. R.; Hoffman, M. Z. *J. Phys. Chem.* **1991**, *95*, 4723. (b) Ohno, T.; Yoshimura, A.; Mataga, N. *J. Phys. Chem.* **1990**, *94*, 4871. (c) Kitamura, N.; Obati, R.; Kim, H.-B.; Tazuke, S. *J. Phys. Chem.* **1989**, *93*, 5764. (d) Navon, G.; Sutin, N. *Inorg. Chem.* **1974**, *13*, 2159.

(4) (a) Ishitani, O.; George, M. W.; Ibusuki, T.; Johnson, F. P.; Koike, K.; Nozaki, K.; Pac, C.; Turner, J. J.; Westwell, J. R. *Inorg. Chem.* **1994**, *33*, 4712. (b) Ishitani, O.; Namura, N.; Yanagadi, S.; Pac, C. *J. Chem. Soc., Chem. Commun.* **1987**, 1153.

(5) (a) Stufkens, D. J. *Coord. Chem. Rev.* **1990**, *104*, 39. (b) Balk, R. W.; Stufkens, D. J.; Oskram, A. *Inorg. Chim. Acta* **1978**, *28*, 133. (c) Servaas, P. C.; van Dijk, H. K.; Snoeck, Th. L.; Stufkens, D. J.; Oskam, A. *Inorg. Chem.* **1985**, *24*, 4494. (d) Staal, L. H.; Terpstra, A.; Stufkens, D. J. *Inorg. Chim. Acta* **1979**, *34*, 97.

(6) (a) Lees, A. J. *Chem. Rev.* **1987**, *87*, 711. (b) Manuta, D. M.; Lees, A. J. *Inorg. Chem.* **1986**, *25*, 1354. (c) Manuta, D. M.; Lees, A. J. *Inorg. Chem.* **1983**, *22*, 572.

(7) (a) Wrighton, M. S.; Morse. D. L. *J. Organomet. Chem.* **1975**, *97*, 405. (b) Pdungsap, L.; Wrighton, M. S. *J. Organomet. Chem.* **1977**, *127*, 337. (c) Saito, H.; Fujita, J.; Saito, K. *Bull. Chem. Soc. Jpn.* **1968**, *41*, 359.

(8) (a) Shaver, R. J.; Rillema, D. P. *Inorg. Chem.* **1992**, *31*, 4101. (b) Shaver, R. J.; Rillema, D. P.; Woods, C. J. *J. Chem. Soc., Chem. Commun.* **1990**, 179.

0020-1669/95/1334-5578$09.00/0

resolution spectroscopy.[9–13,15] In Ir^{III} and Rh^{III} cyclometallated systems, the lowest excited state has been identified as predominately ^{3}LC at low temperature with a significant admixture of ^{1}CT arising from spin–orbit coupling in the case of Ir^{III}.[14] In the absorption spectra of [Rh(ppy)$_2$(bpy)](PF$_6$) and [Ir(ppy)$_2$(bpy)](PF$_6$) (ppy = 2-phenylpyridyl anion), metal–ligand stretching vibrations typical of a CT electronic transition appear as vibrational side bands of the nominally assigned ^{3}LC origin. The intensity of these vibrational side bands tracks the relative degree of mixing between the CT and LC excited states as predicted for a dipole intensity stealing mechanism.[10] The admixture of CT into LC can have dramatic effects on the observed excited state decay and optical properties of a transition metal complex. The information contained in the optical spectra of these complexes is very rich, and it can be used to elucidate the nature of the lowest excited state.

Recently, the application of Re^I organometallic species in supramolecular systems designed for photoinduced charge separation and catalysis has attracted attention.[1–4] Application of solid state optical spectroscopic techniques at cryogenic temperatures for the analysis of the fundamental photophysical properties of Re^I organometallic species in the solid state have received little attention. Spectroscopic identification of the lowest excited state in Re^I carbonyl complexes in solution has been difficult, and in some instances dual emission arguments have been implemented to explain experimental results.[2d] In the series [Re(CO)$_3$(LL)(L′)]$^+$ (LL = bpy, phen, etc.; L′ = py, PPh$_3$, etc.), it has been postulated that the lowest CT state lies close in energy to the LC state and dominates emission at 298 K, while the LC state dominates at cryogenic temperatures (<100 K).[1,2] The temperature dependence is described by a thermally activated population of the CT state. The absorption and emission properties of [Re(bpy)(CO)$_4$](OSO$_2$CF$_3$) at room temperature have been interpreted as arising from an emitting ^{3}LC state which is in thermal equilibrium with a lower lying ligand field state. This argument in which the LF state is in equilibrium with a higher lying state has also been used for the interpretation of excited state decay in other [M(LL)(CO)$_4$] systems (M = Cr^0, Mo^0, Mn^I, and LL = bpy, py, phen, etc.).[5] Efficient electron transfer to an acceptor following photoexcitation has been observed for complexes of the type [Re(bpy)(CO)$_4$]$^+$.[8b] The electron transfer could arise either via the LC state, localized on the acceptor bipyridine ligand, or from population of an unassigned CT state at higher energy. Unambiguous identification and characterization of the lowest excited state and exploitation of possible state mixing may significantly enhance the understanding of photoinduced catalytic properties in Re^I organometallic complexes.

The application of high resolution absorption spectroscopy using polarized light to [Re(bpy)(CO)$_4$)](PF$_6$) has allowed a detailed analysis of the electronic transitions in this complex with nominal C_{2v} symmetry.

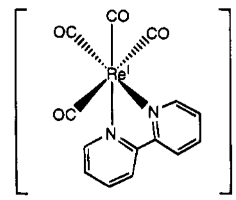

(PF$_6$)

The tetracarbonyl species exhibits well-resolved vibrational structure in the lowest energy absorption band, which is typical of ^{3}LC excitations. On the other hand, it has characteristics typically observed in CT transitions: strong metal–ligand vibrational side bands, a transition moment along the Re→bpy axis, and a luminescence lifetime in the microsecond range at 10 K. This behavior in [Re(bpy)(CO)$_4$](PF$_6$) is assigned as arising from a lowest lying ^{3}LC state which has significant charge transfer character. The lowest energy ^{3}CT transition lies about 5500 cm^{-1} above the first ^{3}LC transition. These transitions show significant polarization effects, and the LC excitation steals intensity from the CT excitation. Mechanisms for intensity stealing form the higher lying CT state and the percentage of CT admixture into the ^{3}LC electronic transition are discussed.

2. Experimental Section

2.1. Synthesis and Crystallization. Starting Materials. The ligand 2,2′-bipyridine (Aldrich) was recrystallized from ethyl acetate prior to use. [Re(CO)$_5$Cl] (Aldrich) and Ag(CF$_3$SO$_3$) (Aldrich) were used without further purification. [Re(CO)$_5$(OSO$_2$CF$_3$)] was prepared as described in the literature and fractionally recrystallized from dichloromethane by the addition of hexane prior to the preparation of [Re(bpy)(CO)$_4$](PF$_6$).[16] All solvents used in preparations were distilled prior to use.[17]

Preparation of [Re(bpy)(CO)$_4$](PF$_6$). The salt [Re(bpy)(CO)$_4$](PF$_6$) was prepared by a procedure analogous to that of Rillema et al. from [Re(CO)$_5$(CF$_3$COOH)].[8b] The triflate salt was converted to the PF$_6^-$ salt by treatment of an acetone solution with a saturated solution of aqueous [NH$_4$](PF$_6$) and recrystallized by slow evaporation of a 1:1 acetone/H$_2$O (v:v) solution at room temperature. Single crystals suitable for crystal structure determination and optical spectroscopy were obtained by slow evaporation of dry acetone at room temperature. The single crystals grow as yellow plates.

Analytical Measurements. FT-IR spectra were recorded in CH$_2$Cl$_2$ solutions. ^{1}H NMR spectra were recorded on a Bruker AC300 spectrometer. Elemental analysis was performed on the single crystals by Ciba-Geigy. Elemental anal. Calcd for ReC$_{14}$H$_8$N$_2$O$_4$PF$_6$: C, 28.05%; H, 1.35%; N, 4.67%; F, 19.02%. Found: C, 27.80%; H, 1.32%; N, 4.61%; F, 19.18%.

2.2. Structure Determination. A single crystal with dimension 0.1 mm × 0.33 mm × 0.40 mm was used for data collection. Intensity data were collected on an Enraf-Nonius CAD4 diffractometer with monochromated Mo Kα radiation using the $\omega/2\theta$ scan technique at room temperature (T = 295 ± 2 K). Cell parameters were obtained from a least squares refinement of 25 centered reflections in the range 10° < θ < 14°. Intensities were corrected for Lorentz, polarization, and absorption (ψ scan method) effects. Scattering factors and anomalous dispersion parameters were taken from the *International*

(9) (a) Colombo, M. G.; Hauser, A.; Güdel, H. U. *Top. Curr. Chem.* **1994**, *171*, 144. (b) Krausz, E.; Riesen, H. *Comments Inorg. Chem.* **1993**, *14*, 323.
(10) (a) Colombo, M. G.; Hauser, A.; Güdel, H. U. *Inorg. Chem.* **1993**, *32*, 3088. (b) Colombo, M. G.; Güdel, H. U. *Inorg. Chem.* **1993**, *32*, 3081.
(11) (a) Giesbergen, C.; Glasbeek, M. *J. Phys. Chem.* ***1993***, *97*, 9942. (b) Zilian, A.; Frei, G.; Güdel, H. U. *Chem. Phys.* **1993**, *173*, 513. (c) Zilian, A.; Güdel, H. U. *Inorg. Chem.* **1992**, *31*, 830. (d) Frei, G.; Zilian, A.; Raselli, A.; Güdel, H. U.; Bürgi, H.-B. *Inorg. Chem.* **1992**, *31*, 4766.
(12) (a) Yersin, H.; Gallhuber, E.; Hensler, G. *Chem. Phys. Lett.* **1987**, *140*, 157. (b) Yamamuchi, S.; Komoda, Y.; Hirota, N. *Chem. Phys. Lett.* **1986**, *129*, 197. (c) Gallhuber, E.; Hensler, G.; Yersin, H. *Chem. Phys. Lett.* **1985**, *120*, 445.
(13) (a) Huber, P.; Yersin, H. *J. Phys. Chem.* **1993**, *97*, 12705. (b) Braun, D.; Gallhuber, E.; Hensler, G.; Yersin, H. *Mol. Phys.* **1989**, *67*, 417. (c) Yersin, H.; Huber, P.; Braun, D. *J. Phys. Chem.* **1990**, *94*, 3560.
(14) Lever, A. P. B. *Inorganic Electronic Spectroscopy*, 2nd ed.; Elsevier: New York, 1984; pp174–178.
(15) (a) Carstens, D. H. W.; Crosby, G. A. *J. Mol. Spectrosc.* **1970**, *34*, 113. (b) Flynn, C. M.; Demas, J. N. *J. Am. Chem. Soc.* **1974**, *96*, 1959. (c) Maeder, U.; Von Zelewsky, A.; Stoeckli-Evans, H. *Helv. Chim. Acta* **1992**, *75*, 1320. (c) Indelli, M. T.; Carioli, A.; Scandola, F. *J. Phys. Chem.* **1984**, *88*, 2685. (d) Nishizawa, M.; Suzuki, T. M.; Watts, R. J.; Ford, P. J. *Inorg. Chem.* **1984**, *23*, 1837.
(16) (a) Trogler, W. C. *J. Am. Chem. Soc.* **1979**, *101*, 6459. (b) Trogler, W. C. *Inorg. Synth.* **1989**, *26*, *113*.
(17) Perrin, D. D.; Armarego, W. L. F.; Perrin, D. R. *Purification of Laboratory Chemicals*, 2nd ed.; Pergamon: Oxford, U.K., 1980.

Table 1. Crystallographic Data for $[Re(bpy)(CO)_4](PF_6)$

formula	$ReC_{14}H_8O_4N_2PF_6$	μ (Mo Kα) (cm^{-1})	70.84
crystal size (mm^3)	0.10 × 0.33 × 0.40	min. transmn factor	0.65
crystal system	triclinic	measd reflecns	4042
a (Å)	9.248(2)	independent reflecns	3879
b (Å)	14.008(2)	R_{int}	0.021
c (Å)	7.604(2)	obsd reflecns (N_o)	3233 [$I \geq 3\sigma(I)$]
V (Å^3)	889.9(3)	$\theta_{min}-\theta_{max}$ (deg)	2–27
d (g cm^{-3})	2.24	hkl range	−11, 11; 0, 17; −9, 9
M_r	599.40	R^a	0.043
temp (K)	298	$R_w{}^b$	0.054
space group	$P\bar{1}$	p^c	0.07
α (deg)	99.65(2)	no. of variables (N_v)	286
β (deg)	108.17(2)	N_o/N_v	11.3
γ (deg)	72.54(1)	max shift/error	0.04
Z	2	GOF^d	1.28
F(000)	564	largest ΔF peak (e Å^{-3})	0.85

[a] $R = \sum||F_o| - |F_c||/\sum|F_o|$. [b] $R_w = [\sum w(|F_o| - |F_c|)^2/\sum wF_o^2]^{1/2}$. [c] $w = 4F_o/(\sigma^2(F_o^2) + (pF_o^2)^2)$. [d] GOF $= \sum||F_o| - |F_c||/(N_o - N_v)$.

Tables for X-Ray Crystallography.[18] Atomic positions for the atoms were determined by Patterson and Fourier transform methods.[19] The structures were refined by full-matrix least squares using anisotropic thermal parameters for all non-hydrogen atoms and isotropic ones for hydrogens.[20] Weights for the last cycle were applied according to the scheme given in Table 1. All calculations were performed using the MolEN system of programs.[19] Positional parameters, displacement parameters, and the unit cell are available as supplemental material.

2.3. Absorption Spectroscopy. Solution spectra were measured on 1 × 10^{-5} M CH_2Cl_2 solutions using 1-cm matched quartz cuvettes on a Cary 5E with a fixed spectral bandwidth of 0.5 nm. Single crystal absorption spectra were recorded on a Cary 5E with a fixed spectral bandwidth of 0.04 nm. The sample and reference beams were plane polarized using a matched pair of Glan–Taylor prisms with the electric vector parallel to one of the extinction directions of the crystal. The crystal, mounted on a copper crystal holder, was cooled in an APD Cryogenics Displex closed cycle helium cryostat fitted with a Scientific Instruments silicon diode 9600-1 temperature controller (accuracy ±1 K).

Orientation of the 1075 μm × 750 μm × 250 μm crystal was conducted using the align command on an Enraf-Nonius CAD-4 diffractometer. The oriented single crystal was affixed on a copper plate over a 500-μm hole using silicon grease. The crystal was aligned under a microscope with the vector of light propagation perpendicular to the *ac* plane. The optical excitation directions in the *ac* plane with respect to the *a* and *c* directions could be determined using a polarization microscope. Absorption measurements were performed with the electric vector of the light beam along the extinction directions.

2.4. Luminescence Spectroscopy. Luminescence experiments were carried out either on polycrystalline samples sealed in a quartz capillary or on a 1 × 10^{-5} M sample dissolved in poly(methyl methacrylate) (PMMA). The samples were cooled in a double-walled helium gas flow tube with temperature control provided by varying the helium gas flow rate (±0.2 K), as described previously.[21] The excitation source was the 355 nm (third harmonic) line from a Quanta-Ray DCR-3 Nd: YAG laser (<5 mJ/pulse). Selective excitations between 440 and 455 nm were performed using Coumarin 2 in a Lambda Physik FL 3002 dye laser–Quanta-Ray DCR-3 Nd:YAG combination. The emission was dispersed by a Czerny–Turner Spex 1402 double monochromator with gratings blazed at 500 nm (1220 grooves/mm) and 200-mm slits. The incident photons were detected by a cooled RCA C31034 photomultiplier coupled to a photon counting system consisting of a Spex DM302 amplifier/discriminator and a Stanford Research SR400 photon counting system. Time resolved emission measurements were conducted using the 20-Hz-pulsed third harmonic (355 nm) of a Nd: YAG as an excitation source with an excitation pulse of <10 ns at <5 mJ/pulse and signal collection at a PMT coupled to a Stanford Research SR430 multichannel scaler. Excited state decay data were fitted to a single-exponential function of the type $I(t) = A + B\exp(-kt)$, using a nonlinear least squares Levenberg–Marquardt routine.[22] The value for A was fixed from dark count measurements under the same experimental conditions.

3. Results

3.1. Crystal Structure. The crystals of $[Re(bpy)(CO)_4](PF_6)$ grow as thin plates, typically with a thickness of 250 μm in which the largest face of the crystal defines the *ac* plane and the narrow face, formed by the long edge of the plate and the edge nearly perpindicular to the *ac* plane, the *bc* plane. The salt crystallizes in the triclinic space group $P\bar{1}$ with cell constants of a = 9.248 Å, b = 14.008 Å, c = 7.604 Å, α = 99.65(2)°, β = 108.17(2)°, γ = 72.54(1)°, and n = 2. The unit cell volume is 889.9(3) Å^3 with a unit cell density of 2.24 g cm^{-3}. Crystallographic data are given in Table 1 with the thermal displacement parameters as a supplemental table (Table 2 of the supplementary material).

The $P\bar{1}$ space group relates two $[Re(bpy)(CO)_4](PF_6)$ subunits in the unit cell by inversion symmetry with a Re–Re nearest neighbor distance of 6.59(1) Å. The PF_6 anions pack in the crystallographic structure by forming sheets between the $[Re(bpy)(CO)_4]^+$ layers when viewed along the *c* axis of the crystal structure (Figure 1 of the supplementary material).

The molecular structure is depicted in Figure 1, with the atom numbering scheme shown. The average Re–N bond distance is 2.17 Å, the average Re–C bond distance for the CO molecules *out of plane*, which are with respect to the bipyridine ligand, 1.93 Å (C_8, C_{10}), and the average *in plane* Re–CO, 2.01 Å (C_7, C_9). The torsion angle between the two N's in the bipyridyl ring is N2–C1–C1′–N2′ is 1.91°. The angle between the CO's are 176.4(3)° for the *out of plane* CO (C8–Re1–C10), and 90.0(4)° for the *in plane* CO (C7–Re1–C9). This is in good agreement with the observed bond distances and bond angles in the crystal structure of the related complex $[Re(bpm)(CO)_4](BF_4)$ (bpm = 2,2′-bipyrimidine), which crystallizes in a monoclinic space group ($P2_1/n$).[8a] Atomic positional parameters for $[Re(bpy)(CO)_4](PF_6)$, bond distances, and bond angles are given in Tables 2 and 3. Positional parameters of the hydrogen atoms and their estimated standard deviation are given in a supplemental table (Table 1 of the supplementary material).

3.2. Absorption Spectra. Absorption spectra of $[Re(bpy)(CO)_4](PF_6)$ at 298.0 ± 0.5 K in CH_2Cl_2 (1.0 × 10^{-5} M) and at 15.0 ± 0.5 K on a single crystal with the light propagation

(18) Cromer, D. T.; Waber, J. T. *International Tables for X-Ray Crystallography*; Kynoch Press: Birmingham, U.K., 1974; Vol. 4.
(19) Fair, C. K. *MolEN. An Interactive Structure Solution Procedure*; Enraf-Nonius: Delft, The Netherlands, 1990.
(20) Johnson, C. K. *ORTEP II: a Fortran Thermal-Ellipsoids Plot Program for Crystal Structure Illustration*; Report ORNL-5138; Oak Ridge National Laboratory: Oak Ridge, TN, 976.
(21) Krausz, E.; Tomkons, C.; Adler, H. *J. Phys. E; Sci. Instrum.* **1982**, *15*, 8910.
(22) Press, W. H.; Flannery, B. P.; Teukolsky, S. A.; Vetterling, W. T. *Numerical Recipes. The Art of Scientific Computing*; Cambridge University Press: Cambridge, U.K., 1986.

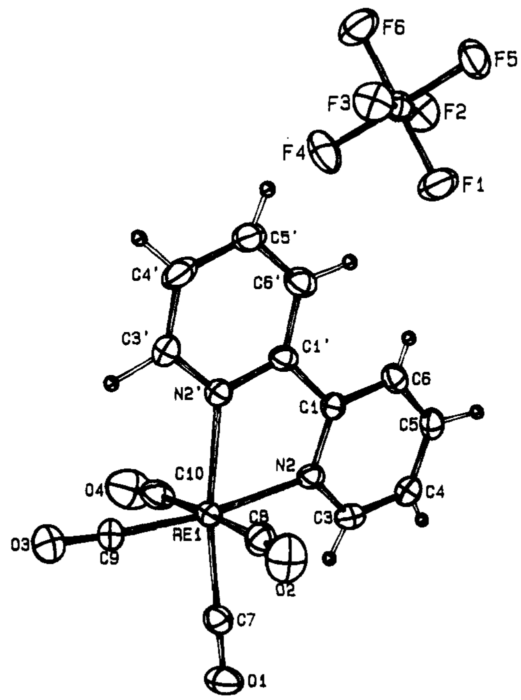

Figure 1. Molecular ORTEP structure of $[Re(bpy)(CO)_4](PF_6)$ showing half the unit cell with thermal ellipsoids at 30% probability level. The atomic numbering scheme is shown.

Table 2. Positional Parameters and Their Estimated Standard Deviations for $[Re(bpy)(CO)_4](PF_6)$

atom	x	y	z	B_{eq}[a]
Re1	0.12349(3)	0.16467(2)	0.33317(4)	2.917(5)
C1	0.0490(8)	0.3832(5)	0.2642(9)	2.8(1)
N2	−0.0131(6)	0.3202(4)	0.3152(8)	2.8(1)
C3	−0.1548(8)	0.3582(6)	0.3513(10)	3.3(1)
C4	−0.2369(9)	0.4566(6)	0.3370(10)	3.6(2)
C5	−0.1760(9)	0.5202(6)	0.2801(10)	3.4(2)
C6	−0.0296(9)	0.4832(5)	0.2451(10)	3.2(2)
C1′	0.2075(7)	0.3389(5)	0.2367(9)	2.8(1)
N2′	0.2723(7)	0.2423(4)	0.2723(8)	3.2(1)
C3′	0.4165(9)	0.1971(6)	0.2508(11)	3.9(2)
C4′	0.4959(8)	0.2440(7)	0.1848(12)	4.5(2)
C5′	0.4304(9)	0.3430(7)	0.1460(11)	4.0(2)
C6′	0.2851(9)	0.3907(6)	0.1744(11)	3.7(2)
C7	−0.0363(9)	0.1092(5)	0.3611(11)	3.5(2)
O1	−0.1314(6)	0.0762(5)	0.3700(9)	5.0(1)
C8	0.0546(9)	0.1285(6)	0.0580(11)	3.6(2)
O2	0.0217(9)	0.1001(5)	−0.0910(9)	5.8(2)
C9	0.270(1)	0.0339(6)	0.3520(14)	4.7(2)
O3	0.3629(9)	−0.0419(6)	0.3675(14)	7.6(3)
C10	0.200(1)	0.1917(7)	0.6093(11)	4.6(2)
O4	0.240(1)	0.2016(7)	0.7660(9)	8.5(3)
P1	0.3298(2)	0.6772(2)	0.2360(3)	3.22(4)
F1	0.1617(6)	0.6540(5)	0.1694(9)	6.0(1)
F2	0.2630(7)	0.7691(4)	0.3676(7)	5.6(1)
F3	0.3954(6)	0.5841(4)	0.1049(7)	5.0(1)
F4	0.3847(7)	0.6050(4)	0.3976(7)	6.1(1)
F5	0.2752(6)	0.7486(4)	0.0717(7)	5.3(1)
F6	0.4972(6)	0.6995(5)	0.2993(9)	6.1(2)

[a] $B_{eq} = (4/3)\sum_i\sum_j\beta_{ij}\mathbf{a}_i\mathbf{b}_j$.

perpendicular to the *ac* plane are presented in Figure 2. The crystal spectrum is scaled by a factor of 50 for clarity of the low energy absorption region. The lowest energy crystal absorption band originating at 22 510 cm^{-1} and exhibiting an extremely rich fine structure is not observable in the solution spectrum. This is due to its low intensity and the broadening of the lines in solution. Even in a PMMA glass at 15 K this lowest energy absorption cannot be observed. The shoulder in the solution spectrum at 28 000 cm^{-1} is also observed as an unstructured transition in the single crystal. The higher energy transitions, >29 500 cm^{-1}, were too intense to be observed in the single crystal.

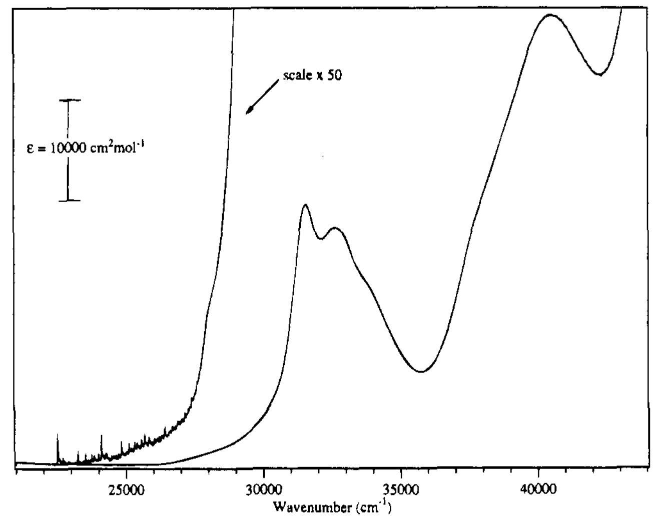

Figure 2. Absorption spectra of $[Re(bpy)(CO)_4](PF_6)$ in solution (1 × 10^{-5} M in CH_2Cl_2) compared to an unpolarized, single crystal absorption spectrum at 15 K with the light propagation perpendicular to the *ac* plane. The single crystal absorption spectrum is enlarged 50 times for clarity in the origin region.

Table 3. Bond Distances (Å) and Angles (deg) for $[Re(bpy)(CO)_4](PF_6)$

Re1−N2	2.169(5)	N2′−C3′	1.343(10)
Re1−N2′	2.181(7)	C3′−C4′	1.361(15)
Re1−C7	1.944(10)	C4′−C5′	1.378(13)
Re1−C8	2.012(8)	C5′−C6′	1.376(11)
Re1−C9	1.923(8)	C7−O1	1.133(12)
Re1−C10	2.005(8)	C8−O2	1.114(10)
C1−N2	1.348(11)	C9−O3	1.144(10)
C1−C6	1.380(9)	C10−O4	1.130(10)
C1−C1′	1.476(10)	P1−F1	1.594(6)
N2−C3	1.355(9)	P1−F2	1.586(6)
C3−C4	1.364(10)	P1−F3	1.590(5)
C4−C5	1.371(14)	P1−F4	1.585(6)
C5−C6	1.390(12)	P1−F5	1.594(6)
C1′−N2′	1.342(9)	P1−F6	1.582(6)
C1′−C6′	1.382(13)		
N2−Re1−N2′	74.6(2)	C3−C4−C5	119.1(8)
N2−Re1−C7	98.2(3)	C4−C5−C6	119.0(7)
N2−Re1−C8	94.4(2)	C1−C6−C5	119.3(8)
N2−Re1−C9	171.7(4)	C1−C1′−N2′	115.4(7)
N2−Re1−C10	89.2(3)	C1−C1′−C6′	123.5(6)
N2′−Re1−C7	171.0(2)	N2′−C1′−C6′	121.0(6)
N2′−Re1−C8	86.4(3)	Re1−N2′−C1′	116.8(50)
N2′−Re1−C9	97.3(4)	Re1−N2′−C3′	124.2(6)
N2′−Re1−C10	94.6(4)	C1′−N2′−C3′	118.7(8)
C7−Re1−C8	88.7(4)	N2′−C3′−C4′	122.5(8)
C7−Re1−C9	90.0(4)	C3′−C4′−C5′	119.5(8)
C7−Re1−C10	90.7(4)	C4′−C5′−C6′	118.2(9)
C8−Re1−C9	87.2(3)	C1′−C6′−C5′	120.0(7)
C8−Re1−C10	176.4(3)	Re1−C7−O1	177.3(7)
C9−Re1−C10	89.3(4)	Re1−C8−O2	173.9(7)
N2−C1−C6	121.6(7)	Re1−C9−O3	177.0(8)
N2−C1−C1′	115.7(6)	Re1−C10−O4	175.(1)
C6−C1−C1′	122.7(8)	F1−P1−F2	88.9(3)
Re1−N2−C1	117.0(4)	F1−P1−F3	90.4(3)
Re1−N2−C3	125.0(6)	F1−P1−F4	90.1(4)
C1−N2−C3	118.1(6)	F1−P1−F5	89.9(3)
N2−C3−C4	122.9(8)	F1−P1−F6	179.2(4)
F2−P1−F3	179.1(4)	F3−P1−F5	90.3(3)
F2−P1−F4	90.5(3)	F3−P1−F6	88.9(3)
F2−P1−F5	90.3(3)	F4−P1−F5	179.2(3)
F2−P1−F6	91.9(3)	F4−P1−F6	90.3(4)
F3−P1−F4	88.9(3)	F5−P1−F6	89.8(4)

Polarized room temperature (298 ± 0.5 K) and low temperature (15 ± 0.5 K) single crystal absorption measurements are presented in Figure 3a,b, respectively. The light propagation

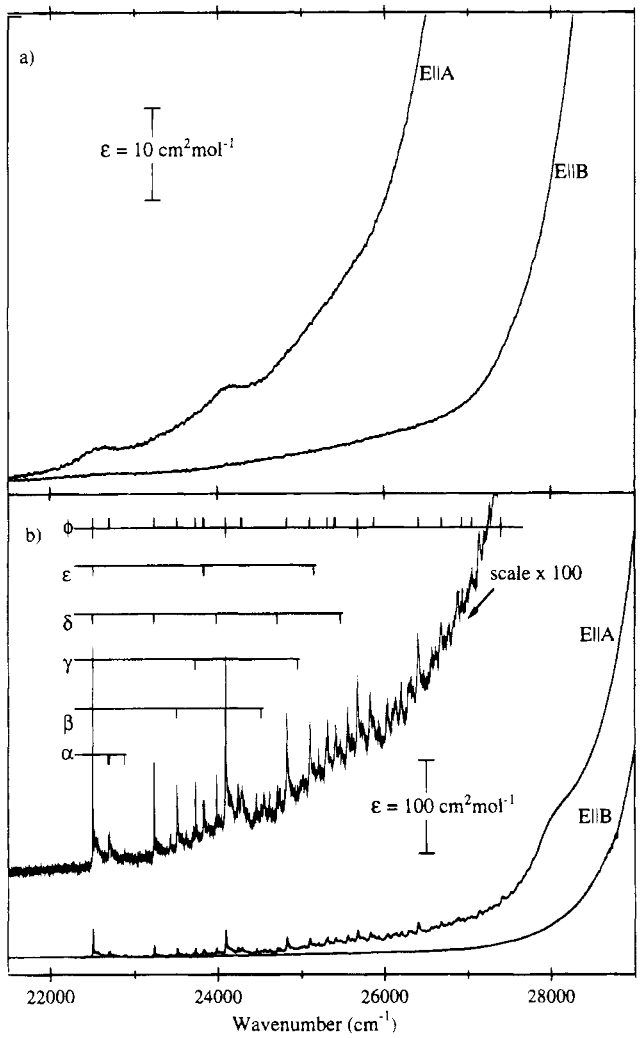

Figure 3. Polarized single crystal absorption spectra of $[Re(bpy)(CO)_4](PF_6)$ at (a) 298 and (b) 15 K. The light propagation vector is perpendicular to the *ac* plane. Polarization directions $E||A$ and $E||B$ refer to the extinction directions of the crystal. Assignment of the progressions in the fundamental vibrational bands, along with the combination bands for the 1590-cm^{-1} mode (ϕ), are shown as an enlarged insert in b.

is perpendicular to the *ac* plane. The polarization directions, *A* and *B*, refer to the experimentally determined extinction directions in the *ac* plane of the crystal. All the absorption bands between 22 000 and 29 000 cm^{-1} are seen to be completely *A* polarized at both temperatures. At room temperature, Figure 3a, three absorptions at 22 500, 24 200, and 26 000 cm^{-1} can be identified in *A* polarization, which upon inspection of the corresponding 15 K spectrum, Figure 3b, can be assigned as arising from a broadening of a series of vibrational progressions. All the sharp features of the low temperature spectrum can be understood as arising from vibrational side bands, overtones, or combination bands of a single electronic origin. A separate broad electronic transition in *A* polarization can be identified at 28 000 cm^{-1} in the low temperature spectrum, which correspond to the 28 000 cm^{-1} shoulder observed in the solution spectrum in Figure 2. Assignments of the progressions in the fundamental vibrations, along with the combination bands for the 1590-cm^{-1} mode (ϕ), are shown as an insert in Figure 3b and further discussed in section 4.2.

In Figure 4 a high resolution spectrum in the region of the electronic origin and the onset of the vibrational progressions is shown with assignments of the first vibrational components. The transitions at 185 (α) and 198 (α') cm^{-1}, which likely arise from a similar vibrational parentage, are not independently labeled. This approximation is also adopted for the γ,γ' and ϵ,ϵ' transitions. The energy and tentative assignment of the origin and vibrational progressions are given in Table 4, along with IR spectroscopic data for $[Re(bpy)(CO)_4](PF_6)$. The tentative band assignments come from the vibrational analysis of $[Ru(bpy)_3](PF_6)_2$ by Kincaid et al.[23] As an insert to Figure 4, the triplet splitting of the electronic origin in $[Re(bpy)(CO)_4](PF_6)$ is shown with a nonlinear least squares fit of a tri-Gaussian function ($f(x)$) using a standard Levenberg–Marquardt routine, eq 1, where a is a constant to correct for base line; b_1, b_2, and

$$f(x) = a + b_1 \exp[-((c_1 - x)/\sigma)^2] + b_2 \exp[-((c_2 - x)/\sigma)^2] + b_c \exp[-((c_3 - x)/\sigma)^2] \quad (1)$$

b_3 are the intensities of the transitions to the three spin sublevels; c_1, c_2, and c_3 are the energies of the three spin sublevels; and σ is the full width at half-maximum (fwhm) for the transitions. The value for a could be determined by a base-line fit; σ was assumed to be the same for the three sublevels (2 cm^{-1}). The three transitions are at 22 507.6, 22 511.2, and 22 514.8 cm^{-1} with an intensity ratio of 1:4:1.2. The overall splitting of the triplet components is thus 7.2 cm^{-1}.

3.3. Luminescence. Figure 5 compares the low temperature (10.0 ± 0.5 K) normalized emission spectra excited at 355.0 nm of a $[Re(bpy)(CO)_4](PF_6)$ single crystal and dissolved in PMMA. The onset of the 15 K crystal absorption spectrum is shown for comparison. The crystal luminescence spectrum exhibits a great deal of well-resolved fine structure, whereas the PMMA bands are inhomogeneously broadened. The crystal spectrum is red-shifted by 200–300 cm^{-1} with respect to the PMMA spectrum and exhibits an energy gap between the onset of the crystal luminescence and the absorption origin. In addition, the fine structure in the crystal luminescence spectrum is much more complex than in the absorption spectrum and shows a very strong temperature dependence upon warming from 15 K. All of these observations are indicative of extensive excitation migration and trapping in the crystal. There are obviously traps of various depths leading to a superposition of several spectra. The luminescence spectrum in PMMA is temperature independent between 10 and 298 K, showing only a broadening of the vibrational progressions and a slight decrease in intensity. The same behavior is observed in the luminescence decay, which is single exponential and essentially temperature independent between 10.0 and 298.0 K: $\tau_{298\,K} = 28.5 \pm 1\ \mu s$; $\tau_{10\,K} = 33.0 \pm 1\ \mu s$.

4. Discussion

4.1. General Properties. The observation of a short solution lifetime ($\tau = 2-3\ \mu s$) and low quantum yield for the room temperature emission in $[Re(bpy)(CO)_4](CF_3SO_3)$ ($\phi_{em} = 0.031$) in CH_2Cl_2 has led to a description in which the LC state is in thermal equilibrium with a LF state.[8b] It is postulated that population of the LF state results in ligand substitution of the CO by the triflate ion due to the close ion-pair condition in the complex. Our investigation of this complex in a crystalline and PMMA environment leads to a more accurate picture of the first excited states. Our data are at variance with the hypothesis of a ligand field state within the first 1000 cm^{-1} from the emitting state. In contrast to the reported excited state ordering in $[Re(bpy)(CO)_4](CF_3SO_3)$, the lowest energy excited state is found to be a ^{3}LC state with some CT character. A higher lying ^{3}CT state can be identified but appears to be unpopulated, and there is no evidence for a LF state.[8]

(23) (a) Mallick, P. K.; Strommen, D. P.; Kincaid, J. R. *J. Am. Chem. Soc.* **1990**, *112*, 1686. (b) Strommen, D. P.; Mallick, P. K.; Danzer, G. D.; Lumpkin, R. S.; Kincaid, J. R. *J. Phys. Chem.* **1990**, *94*, 1357.

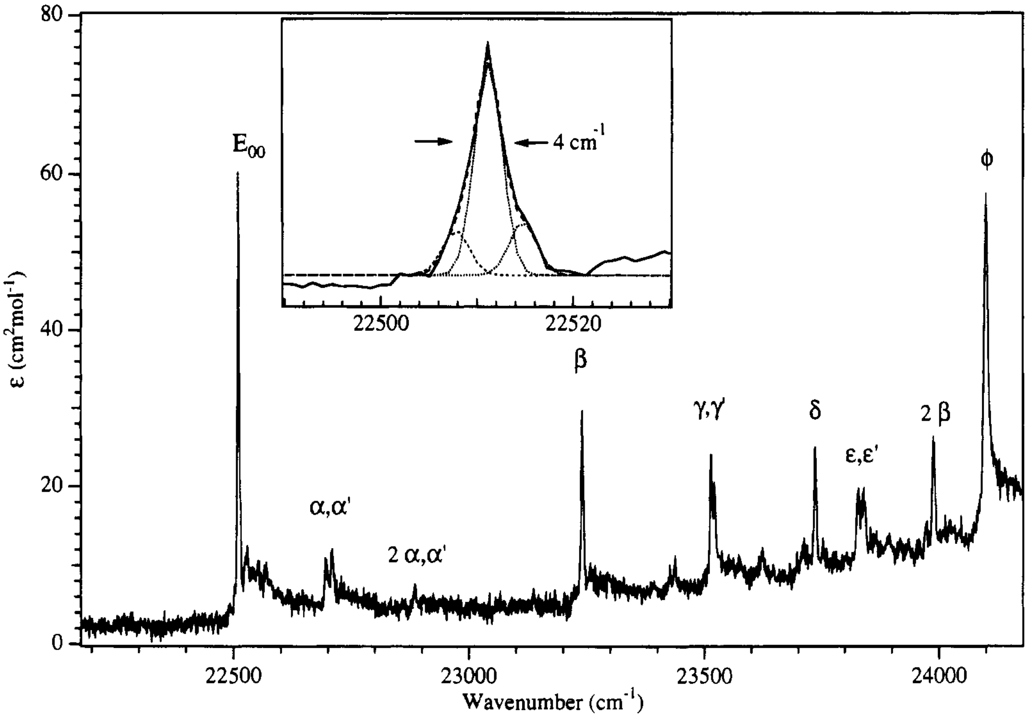

Figure 4. High resolution, single crystal absorption spectrum at 15 K polarized $E||A$ in the region of the electronic origin and the first vibrational components. As an insert the zero-field splitting of the origin is shown with a least squares decomposition into three Gaussian components.

Table 4. Vibrational Side Band Energies and Intensities (*S*) for the Lowest Energy Transition in the Absorption Spectrum of $[Re(bpy)(CO)_4](PF_6)$[a]

absorption band	(*S*) (cm^{-1})	IR band	tenative assignment
α,α′	185, 198 (0.30)		Re−N stretch
		477	
		600	
		631	
		650	
b	731 (0.47)	732	ring bending
		769	
		836	
		858	
		903	
γ,γ′	1005, 1013 (0.65)	964/1027	ring stretch
		1115	
		1126	
		1169	
d	1226 (0.28)	1247	ring stretch
ε,ε′	1318, 1330 (0.32)	1320	ring stretch
		1448	
		1477	
		1499	
f	1590 (1.41)	1607	ring breathing

[a] IR frequencies are shown for comparison, and a tenative assignment is given.

Analysis of the room temperature solution or single crystal absorption spectra of $[Re(bpy)(CO)_4](PF_6)$ in Figure 2 does not allow a clear assignment of the lowest electronic transition. By comparison with the absorption spectra of $[M(bpy)(CO)_4]$ (M = Cr, Mo, W), the intense, broad band at 40 570 cm^{-1} is assigned as a ^{1}LC transition.[6] The overlapping bands at 31 570, 32 600, and 33 800 cm^{-1} are therefore tentatively labeled as ^{1}-CT transitions, although they may also contain some underlying ^{1}LC transitions. The observation of three CT components is consistent with a complex possessing C_{2v} symmetry, resulting in a splitting of the O_h t_{2g} orbitals.[4−6] The broad shoulder observed in the solution spectra at 28 000 cm^{-1} is also observed in the crystal spectrum at 16 K and may arise from either the ^{3}LC or ^{3}CT transition. The significant dipole intensity and band shape allow classification as a ^{3}CT (Re → bpy) transition. This lies about 5500 cm^{-1} to higher energy than the lowest electronic origin.

The observation of a single origin in the highly resolved low temperature absorption spectrum of the lowest energy transition (insert Figure 3b) corroborates the X-ray analysis indicating a single crystallographic site for the Re−bpy moiety in $P\bar{1}$ symmetry. The site symmetry at the Re^I atom in the $P\bar{1}$ space group is C_1. However, the local symmetry at the $[Re(bpy)(CO)_4](PF_6)$ moiety is nearly C_{2v}. This is confirmed by the observation of four CO stretching vibrations for $[Re(bpy)(CO)_4](PF_6)$ at 2120, 2008, 1964, and 1950 cm^{-1} in the infrared spectrum which arise from A_1(out of plane CO, C_8−O_2, C_{10}−O_4), A_1 (in plane CO, C_7−O_1, C_9−O_3), B_1 (out of plane CO, C_8−O_2, C_{10}−O_4), and B_2 (in plane CO, C_7−O_1, C_9−O_3), respectively.[24] Having assigned the ^{3}CT transition around 28 000 cm^{-1}, the highly structured band system between 22 570 and 27 000 cm^{-1} in the low temperature single crystal spectra can be classified as arising from a nominally ^{3}LC transition.

The structured luminescence spectrum in PMMA (Figure 5) shows no significant change in intensity or band shape from 298 to 10 K. The luminescence lifetime in PMMA is single exponential and nearly temperature independent from 298 to 10 K, τ = 28.5 to 33.0 μs, respectively. It follows that the ^{3}LC state is the emitting state with no competition or interference by another state up to room temperature. The presence of a ligand field state within 1000 cm^{-1} from the ^{3}LC origin would lead to an appreciable depopulation of ^{3}LC and thus a quenching of the luminescence and a shortening of the lifetime at room temperature. We can therefore not support the hypothesis of a low lying ligand field state.[8]

We assign the crystal luminescence to traps. Energy migration and excitation trapping is a very common phenomenon in undiluted compounds. The trap sites in $[Re(bpy)(CO)_4](PF_6)$ exhibit a vibrational side band pattern similar to the intrinsic pattern observed in the absorption spectrum. They are thus molecular species containing the Re−bpy group, most likely $[Re(bpy)(CO)_4]^+$ complexes in slightly irregular environments.

(24) Orgel, L. E. *Inorg. Chem.* **1962**, *1*, 25.

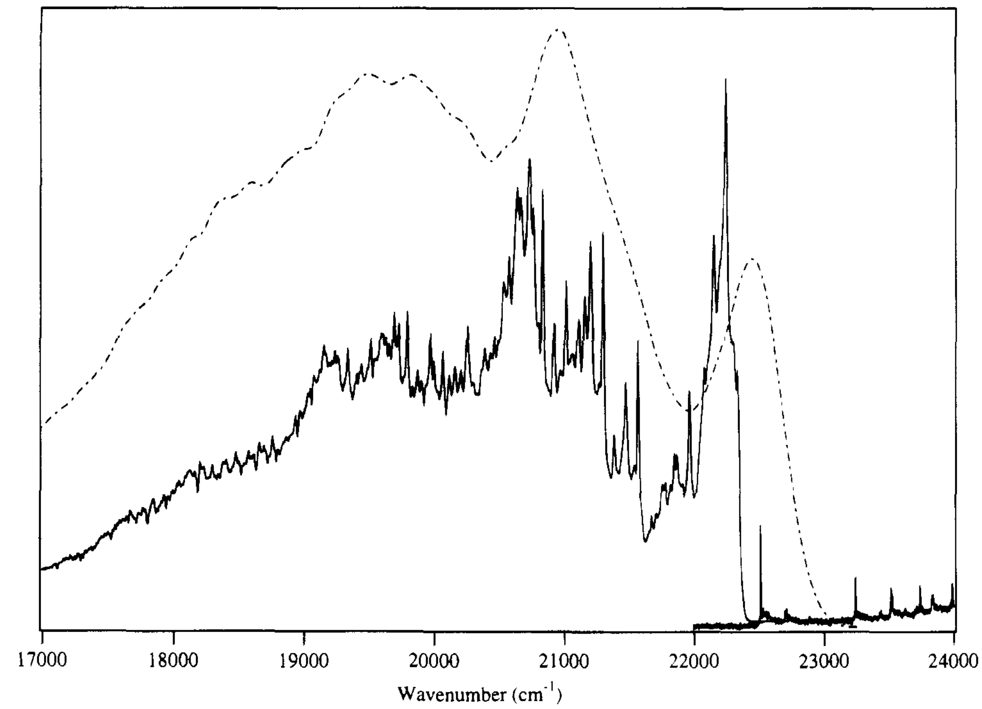

Figure 5. 10 K luminescence spectra of [Re(bpy)(CO)$_4$](PF$_6$) (a) as a single crystal (—) and (b) from a sample dissolved in PMMA (— • —) (λ_{ex} = 355.0 nm). The onset of the crystal absorption origin is shown for comparison.

Their concentration can be in the parts per million range, if the rate constant for energy transfer between neighboring complexes in the crystal is on the order of 10^8 s^{-1} or larger, as estimated in the related complex [Rh(ppy)$_2$(bpy)](PF$_6$). A detailed analysis of the extrinsic trap behavior in the single crystal will be presented in a later manuscript.[25]

4.2. Vibrational Fine Structure of the Absorption Spectrum. A tentative assignment for the six vibrational progressions indicated in Figure 3 is given in Table 4. The higher lying modes (500–1600 cm^{-1}) are assigned to C–C, and C–N stretching modes and mixed stretching–torsional modes of the bipyridine based on the full normal coordinate analysis of [Ru(bpy)$_3$]$^{2+}$ by Kincaid et al. and by comparison to the IR active modes for [Re(bpy)(CO)$_4$](PF$_6$) are listed in Table 4.[23] The dominant ring-breathing mode appears at 1590 cm^{-1}. The Huang–Rhys factor S is determined by the intensity distribution within a given progression (i) by the following equation

$$S_i = n(I_n/I_{n-1}) \qquad (2)$$

where n designates the member in the progression. Its value is 1.45 for the 1590-cm^{-1} progression, which is similar to the observation of such modes in CT excitations and much larger than is typically observed for LC excitations.[9–13,29] For the ^{3}LC excitation of bpy in durene, an S value for the combined 1586-/1606-cm^{-1} mode of ~0.14 is observed.[26]

Several vibrational components of considerable intensity can be identified which are typically found in CT excitations. The α,α′ side bands at 190, 210 cm^{-1} arise from Re–N$_{bpy}$ stretching modes. Very similar metal–ligand vibrations (<300 cm^{-1}) have been identified for the lowest ^{3}CT state in [Os(bpy)$_3$]$^{2+}$ at 190 and 211 cm^{-1} and in [Ni(Cl)$_2$bpy] at 228 cm^{-1}.[13,27] The observation of relatively strong metal–ligand vibrational side bands in [Pd(thpy)$_2$] (thpy = 2-(2-thienyl)pyridine anion) and in [Pt(thpy)$_2$] between 200 and 300 cm^{-1} have been used to assign the lowest electronic transition as a ^{3}CT.[28] It was observed in these Pd^{II} and Pt^{II} materials that the intensity of the metal–ligand mode with respect to the intensity of the electronic origin in the luminescence spectra increased as the spin–orbit coupling increased and as the CT character of the lowest electronic state increased.[28] In the isoelectronic complex, [Re(bpy)(CO)$_3$CN], the Re–N$_{bpy}$ stretching mode has been identified at 178 and 214 cm^{-1} by resonance Raman experiments.[29] Recent investigations of [Ir(thpy)$_2$(bpy)](PF$_6$) doped into [Rh(ppy)$_2$(bpy)](PF$_6$) have revealed similar metal–ligand vibrations at 274 and 376 cm^{-1} (S ~ 0.21) which are only barely visible in the equivalent Rh^{III} complexes (S < 0.1). In the same host lattice, [Ir(ppy)$_2$(bpy)$_2$](PF$_6$) exhibits greater intensity (S ~ 0.26) for the metal–ligand (M–L) mode at 243 cm^{-1}. In the case of the Ir^{III} system the strength of the ν_{M-L} vibrations was correlated to the degree of the admixture of CT character into the LC state.[10] Surprisingly, for a nominal ^{3}LC transition, the α,α′ vibrational progression has significant intensity with a Huang–Rhys factor of 0.30 in [Re(bpy)(CO)$_4$](PF$_6$). The observation of a large Huang–Rhys factor for the M–L vibration in the Re^I complex points to a significant degree of coupling between the ^{3}LC transition and higher lying CT transitions.

At >2000 cm^{-1} no side bands can be identified that correspond to CO stretching vibrations. If the CO vibrations were coupled to the lowest electronic transition, CO vibrational side bands would be predicted. In the case of [Re(bpy)(CO)$_3$Cl], the bpy ring bands in the Raman spectrum show a shift to longer wavelengths due to vibronic coupling of the CO to the MLCT excited state.[29] Evidence for coupling of the CO modes has been observed in the transient excited state Raman and transient infrared spectra for the CT state in [Re(CO)$_3$(bpy)(Cl)].[29] The lack of CO modes and the highly structured vibrational patterns are consistent with the ^{3}LC assignment for the lowest electronic transition in the title compound.

(25) Strouse, G. F.; Güdel, H. U. Manuscript in preparation.
(26) Okabe, N.; Ikayama, T.; Azumi, T. *Chem. Phys. Lett.* **1990**, *165*, 24.
(27) (a) King, E.; Lindner, E. *Spectrochim. Acta* **1972**, *28A*, 1393. (b) Clark, R. J. H.; Williams, C. S. *Spectrochim. Acta* **1967**, *23A*, 1055.
(28) Yersin, H.; Huber, P.; Wiedenhofer, H. *Coord. Chem. Rev.* **1994**, *132*, 35.
(29) Schoonover, J. R. Private communication.

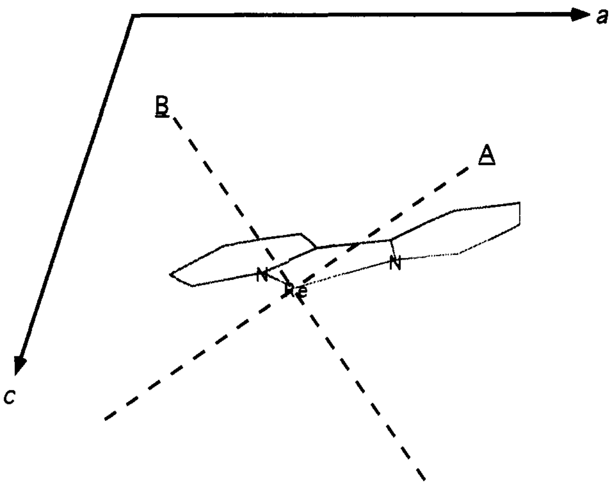

Figure 6. Crystallographic projection of a Re(bpy) unit perpendicular to the *ac* plane. The *A* and *B* directions are experimentally determined optical extinction directions.

4.3. Transition Moment of the Lowest Energy Excitation. Besides the highly resolved fine structure, there is another very important piece of information in the polarized single crystal absorption spectrum of Figure 3. It is the polarization behavior. From the polarization behavior it is possible to deduce information about the optical quality of the crystal and the nature of the observed electronic transitions. All the sharp absorption bands between 22 500 and 28 000 cm^{-1} are more intense when the electric vector is parallel to extinction direction A ($E||A$) than when the electric vector is parallel to extinction direction B ($E||B$) by a factor of >100:1. The high optical quality of the crystal is demonstrated by the remarkably small degree of depolarization of the light beam which occurs when the light crosses the faces of the crystal.

The observation that each of the sharp absorption bands of the system has the same polarization ratio is a very strong indication that they all arise from the same electronic transition. The rich fine structure arises from vibrational side bands of a single electronic origin involving totally symmetric modes of the complex. This assignment is supported by the fact that overtone and combination bands of the fundamental vibrations (α to ϕ) are observed in the side band vibration pattern, Figure 3b.

The complete $E||A$ polarization is more difficult to interpret. The polarization direction A is an extinction direction of the *crystal*, but the polarization properties of a given electronic transition are dictated by the relative orientation of the electric vector and the principle axes of the individual *complex*. From the experimental polarization data, it can be concluded that all the molecules in the crystal lie with their principle axes parallel or antiparallel. In addition, in this projection the crystal A direction must coincide with one of the principle axes of the complex. In order to confirm this and determine which molecular axis coincides with the A optical axis, the optical data and the crystal structure information must be connected. For this purpose the optically determined A and B extinction directions in the *ac* plane were correlated to the *a* and *c* axes of the crystal with the use of a polarization microscope and a four-circle diffractometer. The result is shown in Figure 6. The Re−bpy part of the complex is projected onto the *ac* plane, and the extinction directions A and B are drawn from the Re atom. In this projection A coincides with the C_2 axis of the complex. Using the nomenclature of the free bpy ligand, the C_2 axis within the molecular plane is the short axis (SA). The long axis (LA) is in the plane of the bpy ligand perpendicular to the SA, and the out of plane axis (OP) is perpendicular to the bpy plane. The coincidence of the molecular SA and the crystal A direction in the projection of Figure 6 is not exact. There is an angle of 3.5° between the two directions in the *ac* plane. However, this mismatch is irrelevant for the following reason.

The transition moment $\vec{m}$ of an electronic transition is defined in terms of the principle axes of the complex; i.e., it has the components m_{SA}, m_{LA}, and m_{OP}. The absorption intensity (A) induced by the electric vector $\vec{E}$ of the radiation field is given by

$$A \propto |\vec{m}\cdot\vec{E}|^2 \qquad (3)$$

If $\vec{E}$ is exactly parallel to SA, the intensity is determined by $(m_{SA})^2$.[30] If there is an angle α between $\vec{E}$ and SA, the intensity from $(m_{SA})^2$ is attenuated by the factor $\cos^2 \alpha$. For $\alpha = 3.5°$ this amounts to the observation of 0.9963 of the SA intensity. In other words only 0.4% of the SA intensity is expected in the crystal B polarization, in excellent agreement with the experiment.

For the lowest energy optical excitation in [Re(bpy)(CO)$_4$](PF$_6$) we conclude that the transition moment has only one nonzero component, m_{SA}. Inspection of Figure 3 further reveals that the same conclusion can be drawn for the broad ^{3}CT transition at 28 000 cm^{-1}. Although we cannot experimentally observe the polarization for the ^{1}CT transition, we assume the polarization is the same as that of the ^{3}CT and lies along the SA, as predicted theoretically.[35] This information about the principle axis of the transition moment in the complex is very important for an understanding of the relevant intensity mechanisms; see section 4.4. It can only be obtained from measurements on single crystals using polarized light, which is often nontrivial. In addition, the spectroscopic information has to be correlated with the crystal structure by an additional X-ray experiment. We feel that in some selected instances this considerable effort is justified, because the information thus obtained allows a deeper analysis of electronic structure in the photocatalytically relevant first excited states of such d^6 chelate complexes.

4.4. Mixing of LC and CT Character. The absorption and luminescence data are consistent with an assignment of the lowest energy electronic transition as a ^{3}LC ($\pi \rightarrow \pi^*$) on bpy. The broad transition around 28 000 cm^{-1}, i.e., about 5500 cm^{-1} higher in energy, can be tentatively assigned to the lowest ^{3}CT (Re^{I} → bpy) excitation. This very simple picture needs some refinement. The well-resolved vibrational fine structure is usually taken as a fingerprint characteristic of a ligand-centered transition. It is important to point out that similar sharp vibrational side bands have been reported for the lowest energy excitation of [Os(bpy)$_3$](PF$_6$)$_2$ doped into [Ru(bpy)$_3$](PF$_6$)$_2$.[13] This excitation is normally classified as ^{3}CT. Also, in the spectra of the title complex there are several features which are clear indicators of some CT character. The total oscillator strength is $f_{SA} = 7.0 \times 10^{-5}$ compared to $f_{OP} \sim 9 \times 10^{-10}$ for bpy in durene.[26,31] The same 5 orders of magnitude difference is found in the radiative luminescence lifetimes: 30 μs in [Re(bpy)(CO)$_4$](PF$_6$) and 1.0 s in bpy in durene.[26] In the free ligand the lowest energy transition is OP polarized,[32] while in the title complex it is SA polarized. The total zero-field splitting (ZFS) of the first excited state in [Re(bpy)(CO)$_4$](PF$_6$) is 7.2 cm^{-1}

(30) Piepho, S. B.; Schatz, P. N. *Group Theory in Spectroscopy with Application to Magnetic Circular Dichroism*; Wiley-Intersience: New York, 1983; pp 6−26.

(31) The oscillator strength (f_{ij}) of the ^{3}LC excitation of bpy in durene was estimated from the radiative rates given in ref 26.

(32) (a) Vinodgopal, K.; Leenstra, W. R. *J. Phys. Chem.* **1985**, *89*, 3824. (b) Yagi, M.; Schyler, B. D.; Maki, A. H. *Chem. Phys. Lett.* **1991**, *157*, 209. (c) Suisalu, A. P.; Kamyshnyi, A. L.; Zakharov, V. N; Aslanov, L. A.; Avarmaa, R. A. *Chem. Phys. Lett.* **1987**, *134*, 617.

(insert Figure 4), whereas in the free ligand it is 0.11 cm^{-1}.[26,32] In the $4d^6$ complexes $[Rh(thpy)_2(bpy)](PF_6)$ and $[Rh(bpy)_3](PF_6)_3$, in which the first excited state is also a nominal ^{3}LC state, ZFS values of 0.144 and 0.132 cm^{-1} have been observed by ODMR measurements.[9a,33,34] Estimated values for the ZFS of the nominal ^{3}LC state from luminescence and excitation data for the $5d^6$ complexes $[Ir(thpy)_2(bpy)](PF_6)$ and $[Ir(ppy)_2(bpy)](PF_6)$, are ~5 and ~10 cm^{-1}, respectively.[9a] The α to ϕ vibrational side bands in $[Re(bpy)(CO)_4](PF_6)$ have Huang–Rhys factors ranging from 0.28 to 1.41 in the high resolution absorption spectrum, as shown in Figure 4. In the phosphorescence spectrum of bpy in durene side band intensities corresponding to less than 0.13 are observed.[26,32] The α vibrational side bands are particularly typical of CT excitations. α being a metal–ligand vibration, its side band intensity is directly related to the CT character of the transition. There is of course nothing comparable in the spectrum of the free ligand. In the absorption spectra of $[Rh(thpy)_2(bpy)](PF_6)$ and $[Ir(thpy)_2(bpy)](PF_6)$, the α vibrational side band has an estimated Huang–Rhys factor of <0.1 and 0.21, respectively, compared to 0.30 in $[Re(bpy)(CO)_4](PF_6)$.

All this evidence points to some CT character in the first excited state of $[Re(bpy)(CO)_4](PF_6)$. By the application of a simple model, the extent of LC–CT mixing can be theoretically estimated. The results will be compared with the experimental data of $[Re(bpy)(CO)_4](PF_6)$, and the observed trends in the series $[Rh(thpy)_2(bpy)](PF_6)$, $[Re(bpy)(CO)_4](PF_6)$, and $[Ir(thpy)_2(bpy)](PF_6)$ will be rationalized.

Following the arguments of Komoda et al., the first $\pi \rightarrow \pi^*$ excited state of the bpy molecule is a $^3B_2$ in C_{2v} point symmetry.[34] This is split into the three ZFS sublevels, T_x, T_y, and T_z transforming as A_1 , A_2, and B_1. In the complex $[Re(bpy)(CO)_4](PF_6)$ the C_{2v} point symmetry of the free ligand is retained. In this point group the three possible d $\rightarrow \pi^*$ CT excitations transform as B_1, B_2, and A_1. The triplet sublevels can only mix with CT levels of the same representation. Thus, it is possible for the $T_x(A_1)$ and $T_z(B_1)$ sublevels of the ^{3}LC state to mix with the corresponding levels of higher lying CT states.

Among the allowed CT excitations those polarized along the metal–ligand direction have been shown by overlap arguments to carry the most intensity.[35] SA polarized CT transitions are the most efficient source of intensity for the ^{3}LC transitions in the stealing mechanism described above. We thus expect a dominant $T_x(A_1)$ component in SA polarization, in agreement with our observation for $[Re(bpy)(CO)_4](PF_6)$ and the complexes $[Rh(thpy)_2(bpy)](PF_6)$ and $[Ir(thpy)_2(bpy)](PF_6)$. In contrast, the intensity of the free ligand bpy occurs by a completely different mixing mechanism, namely, with ^{1}LC excitations, and the resulting dominant intensity is OP polarized.[32]

The mixing of CT character into the lowest energy ^{3}LC states is usually formulated in terms of the spin–orbit coupling operator H_{so} as follows:

$$I_{^3LC} = I_{^1CT}\left(\frac{\langle ^3LC|H_{so}|^1CT\rangle}{E_{^1CT} - E_{^3LC}}\right)^2 + I_{^3CT}\left(\frac{\langle ^3LC|H_{so}|^3CT\rangle}{E_{^3CT} - E_{^3LC}}\right)^2 \qquad (4)$$

where E and I denote the energy and intensity of the transition, respectively.[11a,14] From the absorption spectrum in Figure 2 we estimate a ratio $I_{^1CT}/I_{^3CT}$ of approximately 100. The ratio of the denominators for the two terms in eq 4, on the other hand is approximately 3. We conclude that the first term in eq 4 is dominant, and the equation can therefore be approximated as

$$I_{^3LC} = I_{^1CT}\left(\frac{\langle ^3LC|H_{so}|^1CT\rangle}{E_{^1CT} - E_{^3LC}}\right)^2 \qquad (5)$$

Both $I_{^3LC}$ and $I_{^1CT}$ are experimentally accessible from the absorption spectra in Figures 2 and 3. We estimate oscillator strengths $f_{^3LC}$ and $f_{^1CT}$ of 7.0×10^{-5} and 3.7×10^{-2}, respectively. The radiative luminescence decay rate constant (k_r) is another measure of the ^{3}LC transition probability. It is related to the oscillator strength (f_{ij}) by the following equation:

$$1/k_r = 1.5 \times 10^4\left(\frac{1}{f_{ij}}\right)\frac{(c/\nu)^2}{n((n^2 + 2)/3)^2} \qquad (6)$$

where c is the speed of light, ν is the transition frequency, and n is the refractive index (n is estimated to be 1.5).[9a,36] From the observed oscillator strength of the ^{3}LC absorption we calculate a radiative lifetime of 32 μs. This is exactly the measured lifetime of $[Re(bpy)(CO)_4](PF_6)$ in PMMA, and we conclude that the luminescence decay is radiative at all temperatures between 10 and 298 K.

Inserting the experimental values of the ^{3}LC and ^{1}CT energies and intensities into eq 5, we obtain an estimate of the matrix element $\langle|H_{so}|\rangle$ of 261 cm^{-1} for $[Re(bpy)(CO)_4](PF_6)$. On the basis of an analogous analysis, we obtained $\langle|H_{so}|\rangle$ values of 41 and 207 cm^{-1} for the complexes $[Rh(thpy)_2(bpy)](PF_6)$ and $[Ir(thpy)_2(bpy)](PF_6)$, respectively. Qualitatively, these values for the $\langle|H_{so}|\rangle$ matrix element should scale with the estimated spin–orbit parameters for the free ions (ζ): Re^I, ~4000 cm^{-1}; Rh^{III}, ~2000 cm^{-1}; and Ir^{III}, ~6000 cm^{-1}.[37] We do not expect a quantitative agreement, because in $[Rh(thpy)_2(bpy)](PF_6)$ and $[Ir(thpy)_2(bpy)](PF_6)$ the first excited state is localized on the cyclometalating thpy anion ligand which has a much higher σ donor contribution to the chemical bond. The strong ligand influence at the metal center can be seen in the $\langle|H_{so}|\rangle$ matrix element for $[Ir(thpy)_2(bpy)]^+$ compared to $[Ir(thpy)_2(en)]^+$ or $[Ir(ppy)_2(bpy)]^+$, where values of 207, 310, and 182 cm^{-1} are observed, respectively.

Finally, we can try to rationalize the magnitude of the ZFS in the lowest excited state. According to Komoda, using second order perturbation theory, the ZFS can be expressed as

$$ZFS = \langle ^1CT|H_{so}|^3LC\rangle^2\left(\frac{1}{(E_{^3CT} - E_{^3LC})} - \frac{1}{(E_{^1CT} - E_{^3LC})}\right) \qquad (7)$$

where $\langle|H_{so}|\rangle$ is taken from the above estimates, and the energies (cm^{-1}) are obtained experimentally from the absorption spectra in Figure 3.[34] The second order perturbation equation predicts that the ZFS will increase strongly as ζ increases but also as the energy gap between the lowest CT and LC state decreases. Using eq 7, ZFS values of 6.0, 0.04, and 2.6 cm^{-1} are calculated for $[Re(bpy)(CO)_4](PF_6)$, $[Rh(thpy)_2(bpy)](PF_6)$, and $[Ir(thpy)_2(bpy)](PF)_6$, respectively. These are in good agreement with the experimental values of 7.2, 0.144, and 5 cm^{-1}, respectively.[9a]

We conclude that the perturbational approach of Komoda provides a reasonable basis for describing the mixing between LC and CT character in the first excited state of the compound. Using first order perturbation theory and the approximation used above, the wave function ψ' for the lowest electronic state is

(33) Glasbeek, M.; Giesbergen, C. *J. Phys. Chem.* **1993**, *97*, 9942.
(34) Komoda,Y.; Yamamauchi, S.; Hirota, N. *J. Phys. Chem.* **1986**, *90*, 6425.
(35) (a) Day, P.; Sanders, N. *J. Chem. Soc. A* **1967**, 1536. (b) Ceulemans, A.; Vanquickenborne, L. G. *J. Am. Chem. Soc.* **1981**, *103*, 2238.
(36) Imbusch, G. F. Inorganic Luminescence. In *Luminescence Spectroscopy*; Lumb, M. D., Ed.; Academic Press: London, 1978; pp 1–88.
(37) Bendix, J.; Boroson, M.; Schäffer, C. E. *Inorg. Chem.* **1993**, *32*, 2838.

given by

$$\psi' = (1 - a^2)^{1/2}\psi_{^3LC} + a(\psi_{^1CT}) \quad (8)$$

The percentage of ^1CT character mixed into the lowest ^3LC state is given by the coefficient a

$$a = \frac{\langle ^3LC|H_{so}|^1CT\rangle}{E_{^1CT} - E_{^3LC}} \quad (9)$$

which is approximately 3% in $[Re(bpy)(CO)_4](PF_6)$.

5. Conclusion

The photochemical and photocatalytic properties of transition metal complexes can only be properly understood if the relevant lowest excited states are accurately characterized. Photophysical and photochemical measurements at room temperature in solution, i.e., the "natural" environment for photochemistry and catalysis, are very important but often not sufficient for a proper characterization. The present study on $[Re(bpy)(CO)_4](PF_6)$ demonstrates that a thorough spectroscopic investigation in the "artificial" crystal environment at cryogenic temperatures can provide valuable insight into the nature of the first excited states. The main advantages of this environment are four-fold. Competition by complicating photochemical processes is eliminated so that the pure spectroscopic and photophysical properties are accessible. The information content of the spectra is increased by orders of magnitude when fine structure can be resolved. The molecular complexes are spatially oriented in the crystal, and thus, by using polarized light the principle components of the transition moment in the complex can be determined. Multiphonon relaxation processes are suppressed at cryogenic temperatures so that the purely radiative lifetime of the first excited state is observable.

For $[Re(bpy)(CO)_4](PF_6)$ this has led to a very clear picture of the first excited state, which is only in partial agreement with the picture derived from solution experiments at room temperature.[8] The first excited state can be classified as a ^3LC excited state on the bpy ligand. It has about 3% Re → bpy charge transfer character, however. This 3% contamination might appear negligible at first sight. It is definitely not, as evidenced by the increase in oscillator strength for this excitation by 5 orders of magnitude, by its polarization along the Re→bpy axis, by the large Huang–Rhys factors in the vibrational progressions and by the appearance of relatively intense $Re-N_{bpy}$ vibrations in the side band structure.

As suggested previously, the photosubstitution of the complex cannot arise from population of LF states, which lie at least 1000 cm^{-1} to higher energy than the lowest observed excitation. Also, the pure LC transition is not expected to result in perturbation of the electron density at the auxillary ligands. Experimental observation of the influence of the CT excitation on auxillary ligands by transient infrared measurements on $Re(bpy)(CO)_3Cl$ is indicative of the possibility of the participation of the CT excitation in photosubstitution pathways.[29] It is likely that this small degree of charge transfer character in the first excited state is at least partly responsible for the observed photoinduced electron transfer and ligand substitution reactivity of this complex in solution.[1–3] The authors of ref 8 postulated the presence of a lowest energy ligand field excited state to account for the observed luminescence quenching and photochemical behavior. We can definitely rule out the presence of a ligand field state within the first 1000 cm^{-1} of the lowest lying ^3LC state. This knowledge is not based on crystal measurements but on the luminescence properties of $[Re(CO)_4bpy]^+$ in a PMMA glass. On the other hand, the first ^3CT excitation can be clearly identified and characterized in the crystal absorption spectrum. It lies about 5500 cm^{-1} higher in energy than the ^3LC excitation, is also completely polarized in the Re → N_{bpy} direction, and has about 4 times more intensity.

Acknowledgment. We thank the Swiss National Science Foundation for financial support.

Supporting Information Available: Tables of positional parameters and general displacement parameters and a figure of a unit cell viewed along the *c* axis (3 pages). This material is contained in many libraries on microfiche, immediately follows this article in the microfilm version of the journal, and can be ordered from the ACS. See any current masthead page for ordering information.

IC950613Q